Simultaneous occurrence of multiferroism and short-range magnetic order in DyFeO$_3$

Jinchen Wang,[1,2,3] Juanjuan Liu,[1] Jieming Sheng,[1] Wei Luo,[1] Feng Ye,[2,3] Zhiying Zhao,[4,5,6] Xuefeng Sun,[4,5,6]
Sergey A. Danilkin,[7] Guochu Deng,[7] and Wei Bao[1,*]

[1]*Department of Physics, Renmin University of China, Beijing 100872, China*
[2]*Quantum Condensed Matter Division, Oak Ridge National Laboratory, Oak Ridge, Tennessee 37831, USA*
[3]*Department of Physics and Astronomy, University of Kentucky, Lexington, Kentucky 40506, USA*
[4]*Hefei National Laboratory for Physical Sciences at Microscale, University of Science and Technology of China, Hefei,
Anhui 230026, People's Republic of China*
[5]*Key Laboratory of Strongly-Coupled Quantum Matter Physics, Chinese Academy of Sciences,
Hefei, Anhui 230026, People's Republic of China*
[6]*Collaborative Innovation Center of Advanced Microstructures, Nanjing, Jiangsu 210093, People's Republic of China*
[7]*Bragg Institute, ANSTO, Locked Bag 2001, Kirrawee DC NSW 2232, Australia*

We report a combined neutron scattering and magnetization study on the multiferroic DyFeO$_3$, which shows a very strong magnetoelectric effect. Applying magnetic field along the c axis, the weak ferromagnetic order of the Fe ions is quickly recovered from a spin reorientation transition, and the long-range antiferromagnetic order of Dy becomes a short-range one. We found that the short-range order concurs with the multiferroic phase and is responsible for its sizable hysteresis. Our H-T phase diagram suggests that the strong magnetoelectric effect in DyFeO$_3$ has to be understood with not only the weak ferromagnetism of Fe but also the short-range antiferromagnetic order of Dy.

Multiferroic (MF) materials, which possess two or more (anti-)ferroic orders, are topical for both fundamental interest and their application potentials [1–5]. Since the discovery of spontaneous magnetoelectric (ME) coupling in TbMnO$_3$ [6], a lot of materials have been actively explored in hope to realize a mutual control of magnetization or electric polarization using electric or magnetic field. For type-II multiferroics, ferroelectricity has magnetic origin and the study of rare-earth iron oxides ReFeO$_3$ has become a fertile ground for exploring such a multiferroic effect. DyFeO$_3$ has been discovered to have one of the strongest ME couplings [7] and, more recently, a piezomagnetoelectric effect [8]. Electric-field generation and reversal of ferromagnetic moments in a single-component bulk material have been realized in Tb- and Gd-doped DyFeO$_3$ [9]. Multiferroic effects have since been observed also in many similar orthoferrites [10–12].

Research on rare-earth orthoferrites ReFeO$_3$ dates back to 1960s [13–16]. Taking advantage of strong coupling between the Re^{3+} and Fe^{3+} magnetic moments, these materials have shown a vast range of nontrivial magnetism, including solitonic lattice [17], laser induced spin switch [18,19], and unconventional magnetization reversal [20,21]. For DyFeO$_3$, both rare-earth and iron moments develop complex magnetic orders at zero magnetic field. At $T_N^{Fe} \approx 600$ K, the Fe magnetic moments develop a canted antiferromagnetic order with a weak ferromagnetic (WFM) c-axis component due to the Dzyaloshinskii-Moriya interaction and it is denoted as the $G_x A_y F_z$ state in Bertaut's notation [22]. The WFM state undergoes a spin reorientation through a Morin-type transition into the $A_x G_y C_z$ state at $T_R^{Fe} \approx 52$ K [23]. Below $T_N^{Dy} \approx 4$ K, magnetic moments of Dy also form a noncollinear

antiferromagnetic (AFM) order in the $G_x A_y$ state [16]. The multiferroic effect takes place when a magnetic field is applied in the c axis [7]. The field recovers the WFM state and suppresses the Morin-type spin reorientation [24,25]. This recovery of WFM is currently believed to be crucial to the MF effect, from symmetry considerations as well as the proposed exchange striction mechanism [7,9,26,27]. The Dy AFM order is also one of the ingredients in the exchange striction mechanism, but is generally regarded as being field insensitive. So far, no direct experimental evidence exists for the finite-field magnetic phases proposed in the theoretical mechanism. Recent experiments suggested that more complex magnetic behaviors might occur in the low-temperature regime where the MF effect appears [28].

In this work, we establish the magnetic phase diagram of DyFeO$_3$, see Fig. 1, through bulk magnetization and single-crystal neutron diffraction studies in a magnetic field. The WFM phase occupies a large area next to T_R^{Fe} in the phase diagram. Contrary to the current expectation, the AFM long-range order (LRO) of the Dy ions is suppressed by the magnetic field and it is replaced by a short-range order (SRO). The strong multiferroic effect is observed only in the Dy SRO phase. The concurrence of the SRO and MF phases suggests that the mechanism of this remarkably strong ME coupling in the prototype rare-earth orthoferrite DyFeO$_3$ ought to be investigated through the interplay between the weak ferromagnetism of the Fe ions and the antiferromagnetic SRO of the Dy ions.

DyFeO$_3$ single crystals were grown by the floating-zone technique [28]. It is crystallized into an orthorhombic unit cell with $a = 5.261$ Å, $b = 5.489$ Å, $c = 7.542$ Å in the $Pbnm$ (No. 62) space group [29]. The magnetization was measured using a Quantum Design VSM system with the applied magnetic field along the c axis. Neutron diffraction experiments were performed at the Taipan triple-axis spectrometer [30] in
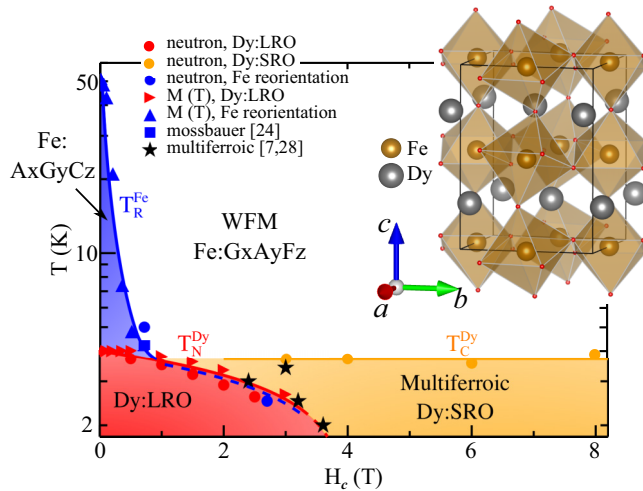
FIG. 1. The phase diagram of DyFeO$_3$ under the c-axis magnetic field. Logarithmic scale is used for temperature. The red symbols denote Dy long-range order temperatures T_N^{Dy}, circles from our neutron measurements and triangles from our magnetization data. The orange circles from our neutron data mark the Dy short-range order temperatures T_C^{Dy}. The blue symbols denote Fe spin reorientation transition temperatures T_R^{Fe}, with blue triangles from our magnetization measurements, blue circles from our neutron measurements, and squares from previous Mössbauer data [24]. Black stars are multiferroic transitions taken from literature [7,28]. (Inset) Crystal structure of DyFeO3 in an orthorhombic *Pbnm* unit cell.

Bragg Institute, Australia Nuclear Science and Technology Organization. A Pyrolytic Graphite filter was put before the sample in the path of the 14.7 meV neutron beam, and a 40$'$ collimator was used after the sample. External fields along the c axis were applied by an Oxford 12-T vertical field cryomagnet. Additional neutron diffraction experiments were conducted at the CORELLI Time-of-Flight spectrometer at Spallation Neutron Source (SNS), Oak Ridge National Laboratory, and the temperature and magnetic field were regulated using a 5T vertical field cryomagnet. During the experiments, magnetic fields were always changed at $T > T_R^{Fe}$ or T_C^{Dy}, and the constant-field temperature dependence studies follow a field cooling (FC) procedure.

The determined phase diagram is shown in Fig. 1. The spin reorientation transition temperature T_R^{Fe} separates two different magnetic structures of Fe, the WFM $G_x A_y F_z$ phase and the spin-reorientation $A_x G_y C_z$ phase. The reorientation temperature T_R^{Fe} is suppressed quickly with magnetic field until the onset of the Dy order below $T_N^{Dy} < 4$ K. Magnetic field below 4 K transforms the LRO of Dy into SRO, while recovers the WFM of Fe at the same critical field. At high fields, Dy ions only form short-range AFM order below T_C^{Dy}, in contrary to generally accepted assumption of a robust Dy AFM LRO in magnetic field [7,9,26,27]. The multiferroic transitions, denoted by black stars, occur only in the coexistence phase of the WFM state of Fe and the SRO state of Dy marked by the orange color in Fig. 1. The detailed results will be present below.

The zero-field magnetic structure is presented in Fig. 2(a), with Figs. 2(b)–2(d) presenting the in-plane view of various
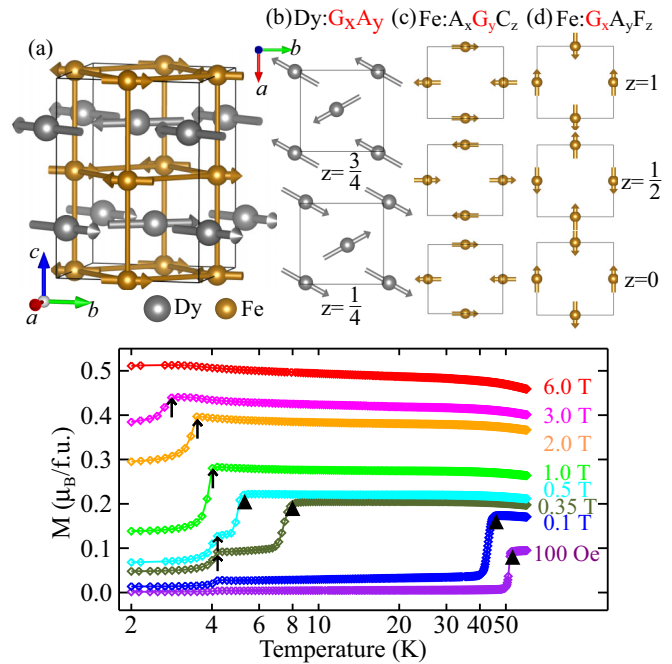

FIG. 2. (a) The schematic magnetic structure of DyFeO$_3$ at zero field. (b) The in-plane view of the $G_x A_y$ configuration of Dy, and (c,d) the $A_x G_y C_z$ and $G_x A_y F_z$ configurations of Fe with a predominant G component. The layers are denoted by the fractional coordinate z. (e) The magnetization data of DyFeO$_3$ under various H_c. Logarithmic scale is used for temperature. The triangles mark the Fe spin reorientation temperature T_R^{Fe}, and arrows the AFM transition temperature T_N^{Dy} of Dy. The $H = 3$ and 6 T data are shifted downwards by 0.07 and 0.32 $\mu_B / f.u.$, respectively.

magnetic configurations. In Fig. 2(e), the magnetization measurements clearly demonstrate two distinct transitions at the low fields. Marked by black triangles, the Fe spin reorientation is observed by a significant decrease of magnetization due to the loss of WFM, consistent with earlier results [23,28]. Further cooling down, another drop of magnetization at around 4 K is observed, which corresponds to the ordering of Dy magnetic moments as will be shown by neutron diffraction data. By applying a small field, T_R^{Fe} decreases rapidly, dropping from 52 K at 100 Oe to 5 K at 0.5 T. This can be understood as the field favors the WFM phase that contains the ferromagnetic component along the c direction. Under fields higher than 0.5 T, only the anomaly relating with the Dy AFM ordering can be resolved. It is getting weakened at higher fields in the magnitude of the anomaly and at the reduced transition temperature, consistent with the weaken Dy AFM LRO observed in neutron diffraction results to be shown in Fig. 3(b).

Now let us turn to the neutron diffraction results. At zero field, both $(0kl)$ and $(hk0)$ scattering planes were investigated at Taipan. With vertical field applying in the c axis, the horizontal $(hk0)$ is the scattering plane at Taipan and CORELLI spectrometers. However, at CORELLI, a finite $\pm 5°$ out of plane coverage can be achieved. Above 4 K, magnetic Bragg scattering is solely from the contribution of Fe ions in the predominantly G-type AFM structure with wave vector (101) or (011) [31]. The G_x to G_y spin reorientation is confirmed by quantitative analysis of peak intensities that are changed
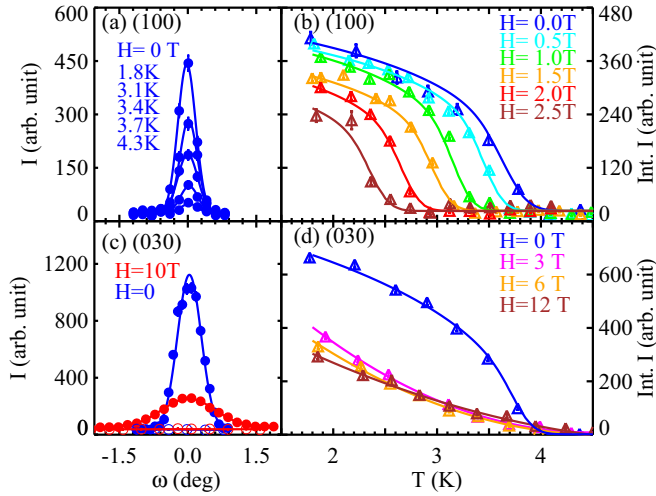
FIG. 3. (a) The rocking scans of the Dy AFM Bragg peak (100) at selected temperatures, $H = 0$ T. (b) The integrated intensity of (100) as a function of temperature under various magnetic fields up to 2.5 T. (c) The rocking scans of the Dy AFM Bragg peak (030) at 0 T and 10 T are compared. The solid circles were measured at 1.8 K, the open ones at 10 K. (d) The integrated intensity of (030) as a function of temperature at selected fields up to 12 T.

around 52 K at $H_c = 0$. The ordering of Dy moments is also confirmed below 4 K, signified by additional magnetic peaks that follow the intensity distribution of the $G_x A_y$ noncollinear AFM configuration [32]. More detailed analysis is presented in Ref. [33]. To measure these different components, we benefit from the fact that the (100) or (300) Bragg peak contains only the A_y component from Dy, the (010) or (030) only the G_x from Dy, and the (200) or (020) from only nuclear contributions. Although the Fe magnetic structures contribute little Bragg scattering in the $(hk0)$ plane, it is possible to find (031) or (301) that is dominated by the Fe signals and within the reach of the experimental setup at CORELLI.

The temperature dependence of Dy magnetic peaks (100) and (030) at various H_c was presented in Fig. 3. Rather than being field insensitive as assumed previously, the AFM of Dy strongly depends on magnetic field. The onset temperature T_N^{Dy} moves from 4 to 2.6 K when H_c ramps up from 0 to 2.5 T, see Fig. 3(b). At higher magnetic fields, a completely different temperature dependence of the peak intensities appears, see Fig. 3(d). The Bragg peaks are significantly broadened, in sharp contrast to the resolution limited peak profiles at zero field, as demonstrated in Fig. 3(c). The broadening of the Bragg peak and the concave shape of the order parameter at $H = 3$–12 T in Fig. 3(d) indicate the high-field phase as a SRO. The broadening occurs on all peaks having Dy magnetic contributions, while pure nuclear peaks remain intact as demonstrated by Bragg peaks in the $(hk0)$ plane in Ref. [33]. The broadening could not be fitted by a small incommensurate peak splitting and is due to a reduced correlation length of the Dy AFM when the magnetic field is sufficiently strong. Corrected for instrument resolution, the intrinsic widths measured on 15 different magnetic peaks fall into the range of $\sigma \sim 0.072 \pm 0.008$ Å^{-1}, resulting in an estimated correlation length $\xi = 4\sqrt{\ln 2}/\sigma \sim 46(5)$ Å in the Dy SRO phase at 1.7 K

and 4 T. By comparing the integrated intensities of the same peaks in LRO phase at 0 T and SRO phase at 4 T, we noticed that the ratio of I_{LRO}/I_{SRO} is about the same for all peaks we have measured. Thus the relative intensity distribution is not altered, and the same $G_x A_y$ correlation is likely maintained for the Dy ions in the SRO phase. The onset temperature T_C^{Dy} for SRO is about 4 K and shows little field dependence all the way up to 12 T, see Fig. 3(d).

The magnetic moment of the Dy ion is as large as $gJ \sim 10\mu_B$, and the exchange energy between Dy ions scales with $k_B T_N^{Dy}$. At $H_c = 6$ T, the magnetic energy of full Dy polarization $gJH_c \sim 10k_B T_N^{Dy}$. From this point of view, it would be difficult for the Dy ions to maintain the AFM order at such a high field. Indeed, such magnetic polarized states have been observed in GdFeO$_3$ with the application of a field at about 3 T [10], close to the LRO breaking down field in our sample. However, the ground state of Dy^{3+} in DyFeO$_3$ is strongly Ising type as in the well studied DyAlO$_3$ [23,32,34,35] and the easy axis lies in the ab plane.[1] The magnetization at 6 T is still less than 1 $\mu_B/f.u.$ in both the paramagnetic and SRO states (see Fig. 2), in contrast to the fully polarized 7 $\mu_B/f.u.$ in GdFeO$_3$. This may explain why the magnetic field is capable of breaking down the LRO but is not able to fully polarize the moment, eventually yielding a SRO. The competition between crystal field anisotropy, exchange interaction and Zeeman energy and their coupling to lattice degrees of freedom must be critical for the understanding of the experiment observations and the ME effect. In any case, the break-down of LRO in DyFeO$_3$ observed in our experiments challenges the theory that the $G_x A_y$ AFM structure of Dy remains unchanged under applied magnetic field and the MF transition is a result of the Fe spin reorientation alone.

In Fig. 4, we show field dependence of the (030) Bragg peak, which is solely from the Dy ordering, the (020) solely from nuclear origin, and the (031) that has mixed contributions from the Dy and Fe magnetic orders, but the Fe contribution gets much boosted after reorientation transition and dominates the intensity. The Dy contribution to (031) is weak in the LRO phase and will become weaker in the high field SRO phase. The field induced LRO to SRO transition is further demonstrated in Figs. 4(a) and 4(b). The magnetic field reduces the correlation length of the Dy AFM order as shown by the broaden peak width and reduces the Bragg intensity. The SRO stabilizes and becomes field independent above the critical field. The Fe reorientation occurs almost simultaneously with the Dy LRO to SRO transition, see Fig. 4(c). This explains why in magnetization measurement only one anomaly remains at high fields in Fig. 2(e). The simultaneity also reveals a strong coupling between Dy and Fe magnetic moments, which is the key ingredient in designing functional magnetoelectric materials [9]. The crystal structure also responds to the magnetic transition. At both 2.5 and 5 K, a bump in the nuclear (020) intensity is observed at the critical field. It is interesting to note that such a magnetostrictive coupling exists

---

[1]The local Ising direction changes between four sublattices following the symmetry of crystal structure, thus forming the in-plane noncollinear AFM structure of Dy.
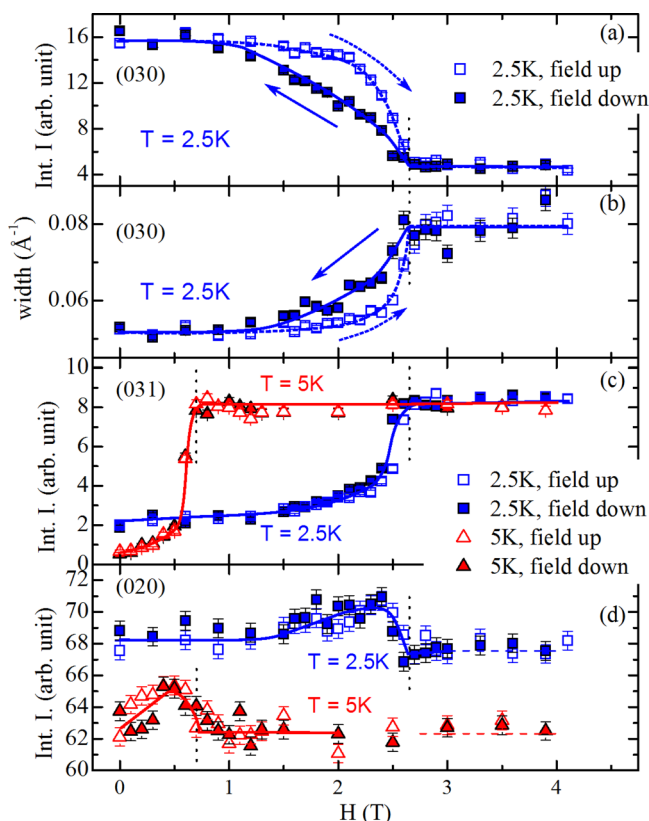
FIG. 4. The field dependence of the integrated intensity of (a) the (030), (c) the (031), and (d) the (020) Bragg peak. (b) The peak width of the (030) Bragg peak represents the full width at half maximum (FWHM) in the radial direction. The field up and down processes are plotted with open and close symbols, respectively, at $T = 2.5$ K (blue) and 5 K (red). The critical fields are marked by the vertical dot lines. The 5-K curve in (d) is shifted downwards from the blue dash line for clarity.

measurements [28] are due to the coupling to the Dy SRO. Complex domain competition has been observed in other orthoferrites ReFeO$_3$ [10], and different tuning rate could lead to different macroscopic response [9]. The hysteresis of the SRO could also play a role in these materials.

The SRO phase is important for the formation of electric polarization in the realization of the MF effect. If zero field cooled into well formed LRO phase, there is no polarization even under finite electric field in the paraelectric state (Fig. 4 in Ref. [28]), until close to the critical magnetic field where we now know that the Dy SRO state has appeared. According to the exchange striction mechanism, the spontaneous electric polarization emerges out of displacements of Dy^{3+} ions [7]. Such displacement is likely disfavored by the LRO, and the relaxation into the SRO state could lower the energy. The poling treatment in multiferroic study usually helps to select one favorable domain. It is interesting that in the case of DyFeO$_3$, field cooling also helps to "freeze" the Dy moments into an SRO state and hinders the restoration of LRO even when the field is released.

In summary, in the combined neutron diffraction and magnetization work on DyFeO$_3$, we found that the Fe spin reorientation phase is stabilized by the Dy long-range AFM order, both of which are suppressed by a magnetic field applying in the c axis at $T_N^{Dy}(H_c)$. While the Fe order is replaced by the WFM order, the Dy LRO by the SRO of the same $G_x A_y$ AFM structure of a correlation length $\xi \sim 46(5)$ Å. The shortening of the correlation length and the break-up of the Dy LRO by the field are gradual and show substantial hysteresis. The appearance of the Dy SRO phase and its hysteresis coincide with the appearance and hysteresis of the magnetoelectric effect in this strong multiferroic material. The understanding of this prototype rare-earth orthoferrite multiferroic material ought to be refined by considering the field-induced Dy antiferromagnetic short-range order in addition to the Fe WFM order.

at 5 K without the Dy magnetic ordering. But the multiferroic behavior emerges only when the Dy moments form short-range ordered AFM structure.

Significant hysteresis in DyFeO$_3$ was observed recently in magnetization, polarization, and thermal conductivity measurements under magnetic field [7,28]. A new phase of Fe magnetic order is proposed for the hysteresis region [28]. However, our neutron diffraction results in Fig. 4 clearly show that there is no detectable hysteresis in the Fe magnetic transition. The hysteresis exists only in the Dy LRO-SRO transition. Thus the sizable nonreversible effects in the bulk

[1] S.-W. Cheong and M. Mostovoy, Nat. Mater. **6**, 13 (2007).

[2] R. Ramesh and N. A. Spaldin, Nat. Mater. **6**, 21 (2007).

[3] M. Fiebig, J. Phys. D **38**, R123 (2005).

[4] D. Khomskii, J. Magn. Magn. Mater. **306**, 1 (2006).

[5] Y. Tokura, S. Seki, and N. Nagaosa, Rep. Prog. Phys. **77**, 076501 (2014).

[6] T. Kimura, T. Goto, H. Shintani, K. Ishizaka, T. Arima, and Y. Tokura, Nature (London) **426**, 55 (2003).

[7] Y. Tokunaga, S. Iguchi, T. Arima, and Y. Tokura, Phys. Rev. Lett. **101**, 097205 (2008).

[8] T. Nakajima, Y. Tokunaga, Y. Taguchi, Y. Tokura, and T.-h. Arima, Phys. Rev. Lett. **115**, 197205 (2015).

[9] Y. Tokunaga, Y. Taguchi, T. Arima, and Y. Tokura, Nat. Phys. **8**, 838 (2012).

[10] Y. Tokunaga, N. Furukawa, H. Sakai, Y. Taguchi, T. Arima, and Y. Tokura, Nat. Mater. **8**, 558 (2009).

[11] M. Shang, C. Zhang, T. Zhang, L. Yuan, L. Ge, H. Yuan, and S. Feng, Appl. Phys. Lett. **102**, 062903 (2013).

[12] U. Chowdhury, S. Goswami, D. Bhattacharya, J. Ghosh, S. Basu, and S. Neogi, Appl. Phys. Lett. **105**, 052911 (2014).

[13] W. C. Koehler, E. O. Wollan, and M. K. Wilkinson, Phys. Rev. **118**, 58 (1960).

[14] D. Treves, Phys. Rev. **125**, 1843 (1962).

[15] D. Treves, J. Appl. Phys. **36**, 1033 (1965).

[16] R. L. White, J. Appl. Phys. **40**, 1061 (1969).

[17] S. Artyukhin, M. Mostovoy, N. P. Jensen, D. Le, K. Prokes, V. G. de Paula, H. N. Bordallo, A. Maljuk, S. Landsgesell, H. Ryll, B. Klemke, S. Paeckel, K. Kiefer, K. Lefmann, L. T. Kuhn, and D. N. Argyriou, Nat. Mater. **11**, 694 (2012).

[18] A. V. Kimel, B. A. Ivanov, R. V. Pisarev, P. A. Usachev, A. Kirilyuk, and T. Rasing, Nat. Phys. **5**, 727 (2009).

[19] A. V. Kimel, A. Kirilyuk, P. A. Usachev, R. V. Pisarev, A. M. Balbashov, and T. Rasing, Nature (London) **435**, 655 (2005).

[20] S. Cao, H. Zhao, B. Kang, J. Zhang, and W. Ren, Sci. Rep. **4**, 5960 (2014).

[21] S. J. Yuan, W. Ren, F. Hong, Y. B. Wang, J. C. Zhang, L. Bellaiche, S. X. Cao, and G. Cao, Phys. Rev. B **87**, 184405 (2013).

[22] E. F. Bertaut, in *Magnetism*, edited by G. T. Rado and H. Suhl, Vol. 3 (Academic, New York, 1963).

[23] G. Gorodetsky, B. Sharon, and S. Shtrikman, J. Appl. Phys. **39**, 1371 (1968).

[24] L. A. Prelorendjo, C. E. Johnson, M. F. Thomas, and B. M. Wanklyn, J. Physics C **13**, 2567 (1980).

[25] C. Johnson, L. Prelorendjo, and M. Thomas, J. Magn. Magn. Mater. **15-18**, Part 2, 557 (1980).

[26] T. Yamaguchi and K. Tsushima, Phys. Rev. B **8**, 5187 (1973).

[27] A. Stroppa, M. Marsman, G. Kresse, and S. Picozzi, New J. Phys. **12**, 093026 (2010).

[28] Z. Y. Zhao, X. Zhao, H. D. Zhou, F. B. Zhang, Q. J. Li, C. Fan, X. F. Sun, and X. G. Li, Phys. Rev. B **89**, 224405 (2014).

[29] M. Marezio, J. P. Remeika, and P. D. Dernier, Acta Crystallographica Sec. B **26**, 2008 (1970).

[30] S. A. Danilkin, G. Horton, R. Moore, G. Braoudakis, and M. Hagen, J. Neutron Res. **15**, 55 (2007).

[31] The Dzyaloshinskii-Moriya interaction produces weak ferromagnetism. The weak ferromagnetic contribution of the canted AFM structure is not our focus in this study. We monitored the $G_x A_y F_z$ structure through its strongest G_x component.

[32] R. Bidaux and P. Mériel, J. Phys. France **29**, 220 (1968).

[33] See Supplemental Material at http://link.aps.org/supplemental/10.1103/PhysRevB.93.140403 for additional single-crystal diffraction data and more detailed data analysis.

[34] H. Schuchert, S. Hüfner, and R. Faulhaber, Z. Physik **222**, 105 (1969).

[35] L. M. Holmes, L. G. Van Uitert, R. R. Hecker, and G. W. Hull, Phys. Rev. B **5**, 138 (1972).